



1 **The Ogooue Fan (Gabon): a modern example of deep-sea system on**
2 **a complex sea-floor topography**

3

4 Salomé Mignard, University of Bordeaux, UMR CNRS 5805 EPOC.

5 Thierry Mulder, University of Bordeaux, UMR CNRS 5805 EPOC

6 Philippe Martinez, University of Bordeaux, UMR CNRS 5805 EPOC

7 Thierry Garlan, SHOM

8

9 **Abstract.** The Ogooue deep-sea Fan located in the northeastern part of the Gulf of Guinea expands over more than 550 km
10 westwards of the Gabonese shelf and passes through the Cameroun volcanic line. Here are presented the first study of
11 acoustic data (multibeam echosounder and 3.5 kHz seismic data) and piston cores covering the deep-sea part of this West
12 African system. This study led to the construction of the sedimentary processes map of this area. The overall system
13 corresponds to a well-developed mud-sand rich deep-sea fan, fed by the Ogooue River 'sedimentary load. This system
14 presents the typical morphological elements of clastic slope apron: tributary canyons, distributary channel-levees systems
15 and lobes elements. However, variations on the slope gradient cumulated with the presence of numerous seamounts,
16 including volcanic islands and mud volcanoes, led to a more complex fan architecture and sedimentary facies distribution.
17 In particular, turbidity currents derived from the Gabonese shelf deposit across several interconnected sedimentary sub-
18 basins located on the low gradient segments of the margin. The repeated spill-overs of the most energetic turbidite flows
19 have notably led to the incision of a large distal valley connecting an intermediate sedimentary basin to the more distal
20 lobe area. The sedimentary facies repartition over the fan indicates that pelagic to hemipelagic sedimentation is dominant
21 across the area. Distribution and thickness of turbidite sand beds is highly variable along the system, however turbidite
22 sands preferentially deposit in the bottom of channel-levee systems and on the most proximal depositional areas. The most
23 distal depocenters receive only the upper parts of the flows, which are composed of fine-grained sediments. The Ogooue
24 deep-sea system is predominantly active during periods of low sea-level because canyon heads are separated from terrestrial
25 sediment sources by the broad shelf. However, the northern part of this system appears active during sea-level highstands.
26 This feature is one deeply incised canyon, the Cape Lopez canyon, located on a narrower part of the continental shelf has
27 a different behaviour and receives sediments transported by the longshore drift.

28

29 **Keywords:** Ogooue Fan, Gulf of Guinea, complex seafloor morphology, turbidity currents, sedimentary processes

30

31

32

33

34

35

36



37 **1 Introduction**

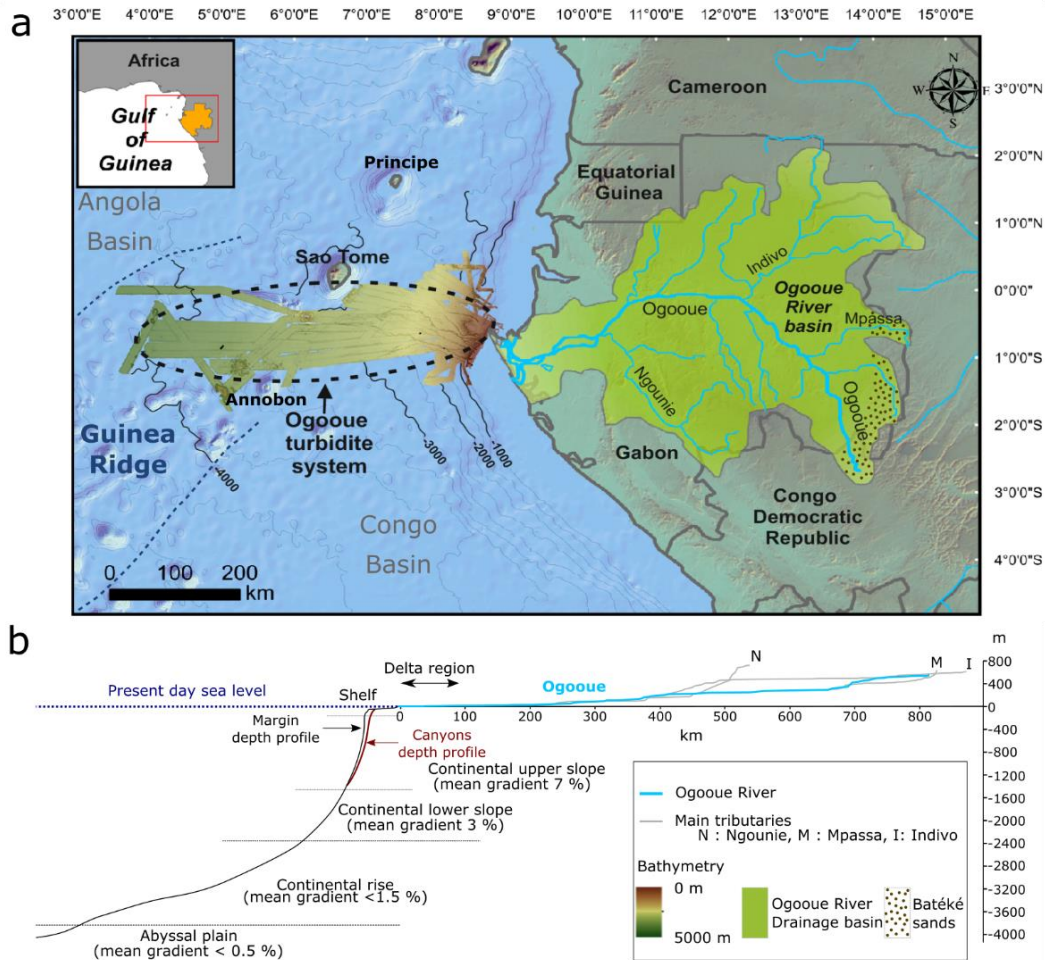
38 The Ogooue Fan is a turbidite system that develops along the central part of the Gabonese margin. Since the Neogene, the
39 West African margin has recorded deep clastic sedimentation forming vast and thick turbidite systems fed by the
40 denudation of the African continent. These deep-sea fans are localized at the outlet of the main rivers, such as the Niger,
41 Congo, Ogooue or Orange River (Anka et al., 2009; Mougamba, 1999; Séranne and Anka, 2005). Due to the presence of
42 important petroleum resources in late Cretaceous and early Tertiary clastic reservoir formations fed by Albian to Turonian
43 source rocks, the geology of the equatorial West African margin province has been widely studied since the early 70's
44 (Brownfield and Charpentier, 2006). Simultaneously, studies of the recent sediment dispersal pattern along this margin
45 have been initiated (Heezen et al., 1964; Weering and Iperen, 1984). These studies of recent and still active systems offers
46 the possibility to observe the continuity between the different features of deep-sea turbidite systems but also to understand
47 the processes and constraints that govern the construction of such sedimentary systems and the facies distribution.

48 Such studies have benefited from the improvement of acquisition tools such as multibeam echosounding and very-high
49 resolution seismic but also from increased frequency of oceanographic cruises allowing to obtain a better cover on the
50 seafloor. In the Gulf of Guinea, many studies focused on the recent Niger (Deptuck et al., 2007, 2003) and the Congo
51 systems (Babonneau et al., 2002; Droz et al., 2003, 1996). On the contrary, the Quaternary sediments of the Gabon passive
52 margin have been relatively poorly studied and the Ogooue deep-sea turbidite system, resulting from the sediment
53 discharge of the Ogooue River, remained for long uninvestigated especially in its deepest parts (Bourgoin et al., 1963;
54 Giresse, 1969; Giresse and Odin, 1973).

55 The survey of the area by the SHOM in 2005 and 2010, thanks to the OpticCongo and MOCOSSED cruises, provided the
56 first dataset on the Ogooue deep-sea turbidite system, from the continental shelf to the abyssal plain. In this paper, we
57 present the first study of the deep-sea Ogooue turbidite system that allows to provide the overall fan morphology as well
58 as its subdivisions but also to understand the sedimentary processes which are involved in the development of the observed
59 sedimentary structures. This study provides an opportunity to investigate a modern deep-sea fan which construction appears
60 largely controlled by bathymetric constrains and by palaeoenvironmental evolution of the West African margin.



61 **2 Geological setting**



62

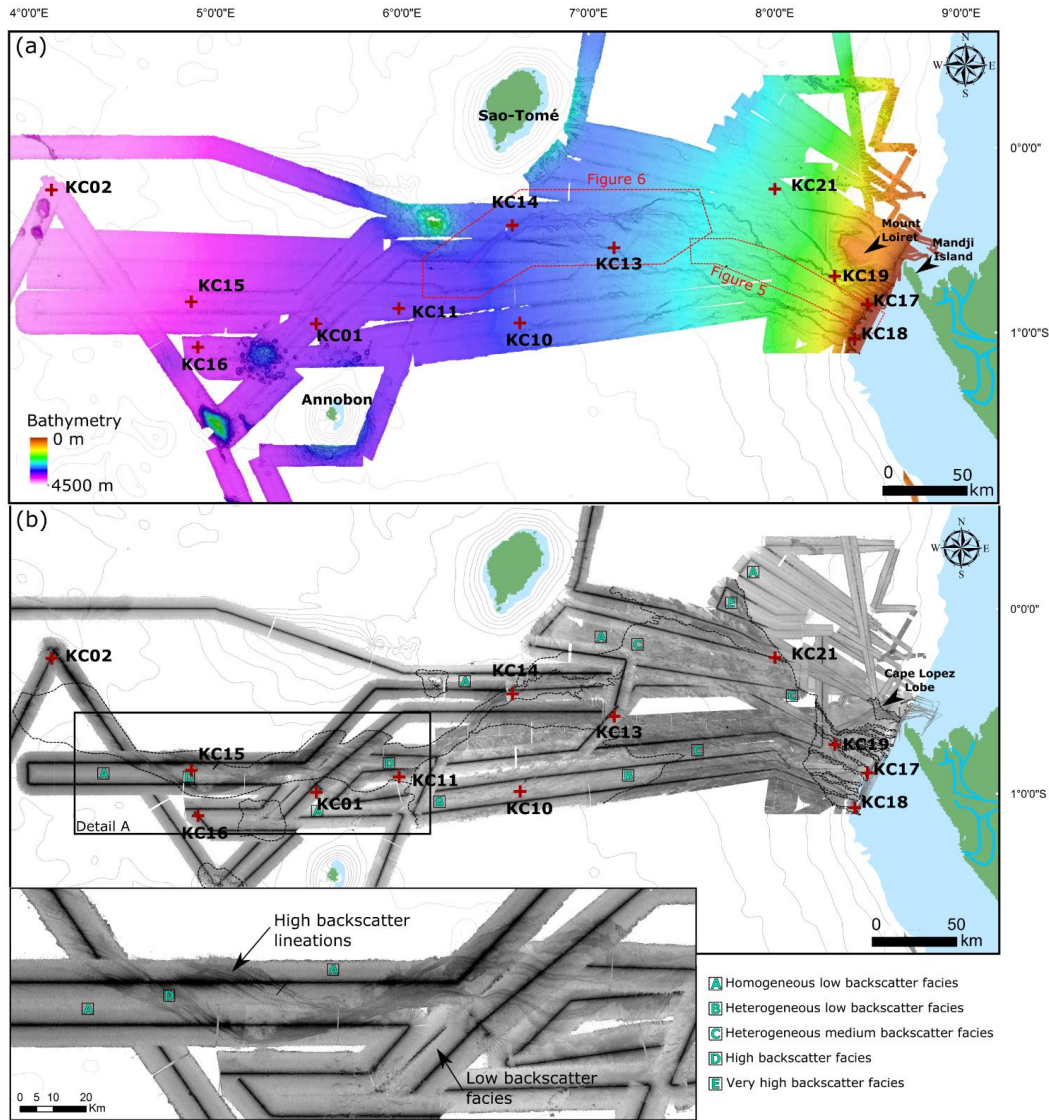
63 **Fig. 1: a) The Ogooue sedimentary system from source (river and drainage basin) to sink (Quaternary turbidite system). b)**
 64 **Channel depth profile of the Ogooue River (blue) and its main tributaries (grey) and mean depth profile along the Gabonese**
 65 **margin.**

66 The Ogooue Fan is located in the northeastern part of the Gulf of Guinea on the Gabonese continental slope. The system
 67 develops on the Guinea Ridge, which separates the two deep Congo and Angola basins. This region is notably characterized
 68 by the presence of several volcanic islands belonging to the Cameroon volcanic line (Fig. 1a). The development of the
 69 Ogooue Fan started during the Late Cretaceous post-rift phase and followed the deposition of a thick Aptian evaporitic
 70 formation which created salt-related deformations of the margin sediments (Cameron and White, 1999; Mougamba, 1999;
 71 Séranne and Anka, 2005; Wonham et al., 2000). The quaternary Ogooue Fan extends westwards over 550 km through the
 72 Cameroon volcanic line. Overall, the modern slope profile is concave upward, similar to that of many other passive
 73 margins. The mean slope gradient evolves from 12% on the very upper slope to <0.5 % in the abyssal plain (Fig. 1b). The
 74 Gabonese continental shelf, which is relatively narrow, can be divided into two sub-parts: the south Gabon margin



75 presenting a SE-NW orientation and the north Gabon margin presenting a SW-NE orientation. The inflection point of the
76 shelf is located at 1°00 S. The South part of the margin is characterized by the presence of numerous parallel straight gullies
77 oriented perpendicular to the slope (Lonergan et al., 2013; Séranne and Abeigne, 1999). On the north Gabon margin, the
78 area located between 1°00 S and the Mandji Island is incised by several canyons that belong to the modern Ogooue turbidite
79 system (Fig. 2a). North of the Mandji Island, the seabed reveals numerous random pockmarks as well as sinuous pockmarks
80 trains. These features are interpreted as the results of fluid migration from shallow buried channels (Gay et al., 2003; Pilcher
81 and Argent, 2007).

82 The Ogooue turbidite system is supplied by the sedimentary load of the Ogooue River, which is third largest African
83 freshwater source in the Atlantic Ocean. Despite the relatively small size of the Ogooue River basin (215,000 km²), the
84 river mean annual discharge reaches 4,700 m³/s due to the wet equatorial climate prevailing on the drainage basin (Lerique
85 et al., 1983; Mahé et al., 1990). The Ogooue River flows on a low slope gradient in a drainage basin where very thick
86 lateritic soils develop over the Congo craton and Proterozoic orogenic belts (Séranne et al., 2008). The estuary area includes
87 several lakes (Fig. 1b) (Lerique et al., 1983). These features contribute to the mainly muddy composition of the particle
88 load of the Ogooue River that is estimated between 1 and 10 M t/yr (Syvitski et al., 2005). The limited portion of sand
89 particles in the river originates mainly from the erosion of the poorly lithified Batéké Sands located on a 550-750 m-high
90 perched plateau that forms the easternmost boundary of the Ogooue watershed (Séranne et al., 2008) (Fig. 1a). On the
91 shelf, recent fluvial deposits consist of fine-grained sediments deposited at the mouth of the Ogooue River (Giresse and
92 Odin, 1973). The wave regime along the Gabonese coast causes sediments to be transported northward. Sedimentary
93 transport linked to longshore drift ranges between 300,000 m³/yr and 400,000 m³/yr (Bourgoin et al., 1963) and is
94 responsible for the formation of the Mandji Island, a sandy spit of 50 km long located on the northern end of the Ogooue
95 Delta (Fig. 2a). Except for the Cape Lopez canyon, located just west of the Mandji Island and which head reaches only
96 5 m water depth (Biscara et al., 2013), the Ogooue turbidite system is disconnected from the Ogooue delta during the
97 present-day high sea-level.



98

Detail A

99

Fig. 2: (a) Detailed bathymetric map of the Ogooue Fan, based on the multibeam echosounder data of the Optic Congo2005 and MOCOSSED2010 surveys. (b) Acoustic imagery of the Ogooue Fan (high backscatter: dark tones; low backscatter: light tones).

100

101

Detail A: close-up of the deepest part of the Ogooue Fan. Red crosses: location of the studied cores.

102

103

104 **3 Material and method**

105 The bathymetry and acoustic imagery of the studied area result from the multibeam echosounder (Seabat 7150) surveys
106 conducted onboard the R/V “*Pourquoi Pas?*” and “*Beautemps-Beaupr e*” during the MOCOSED 2010 and OpticCongo
107 2005 cruises (Guillou, 2010; Mouscardes, 2005) (Fig. 2a). The multibeam backscatter data (Fig. 2b) has been used to
108 characterize the distribution of sedimentary facies along the margin. Changes in the backscatter values correspond to
109 variations of the nature, the texture and the state of sediments and/or the sea-bed morphology (Hanquiez et al., 2007;
110 Unterseh, 1999). On the multibeam echosounder images, lighter areas indicate low acoustic backscatter and darker areas
111 indicate high backscatter. Five main backscatter types are identified on the basis of backscatter values and homogeneity
112 (Fig. 2b). Facies A is a homogeneous low backscatter facies, Facies B is a low backscatter heterogeneous facies, facies C
113 is a medium backscatter facies characterized by the presence of numerous higher backscatter patches. Facies D and E are
114 respectively high and very high backscatter facies. High backscatter lineations are present within facies D.

115 4,500 km of 3.5 kHz seismic lines were collected in the area of the Ogooue Fan during the MOCOSED 2010 cruise and
116 470 km during the Optic Congo 2005 cruise. These data were used to analyze the near-surface deposits. The dataset covers
117 the shelf edge, the slope and the abyssal plain. In this study, the 3.5 kHz echofacies has been classified according to
118 Damuth’s methodology (Damuth, 1980, 1975; Damuth and Hayes, 1977) based on acoustic penetration and continuity of
119 bottom and sub-bottom reflection horizons, micro-topography of the seafloor, and presence of internal structures.

120 The twelve K ullenberg cores presented here were collected during the cruise MOCOSED 2010. Five of these cores have
121 already been presented in (Mignard et al., 2017) (Table 1). Visual descriptions of the cores distinguished the dominant
122 grain size (clay, silty clay, silt, and fine sand) and vertical successions of sedimentary facies. Thin slabs were collected for
123 each split core section and X-ray radiographed using a SCOPIX digital X-ray imaging system (Migeon et al., 1998).
124 Subsamples were regularly taken in order to measure carbonate content using a gasometric calcimeter and grain size using
125 a Malvern Mastersizer S. The stratigraphic framework is based on the previous work of (Mignard et al., 2017)), new AMS
126 ¹⁴C dating and facies correlation to determine the boundary between Marine Isotopic Stage 1 (MIS1) and Marine Isotopic
127 Stage 2 (MIS2). Indeed, the transition from MIS2 to MIS1 in the south-west Atlantic is marked by an abrupt increase in
128 carbonate content (Jansen et al., 1984; Olausson, 1984; Volat et al., 1980; Zachariasse et al., 1984). This feature is recorded
129 in all the deepest cores of this study (Fig. 3).

130

131

132

133

134

135

136

137

138

139

140

141

142

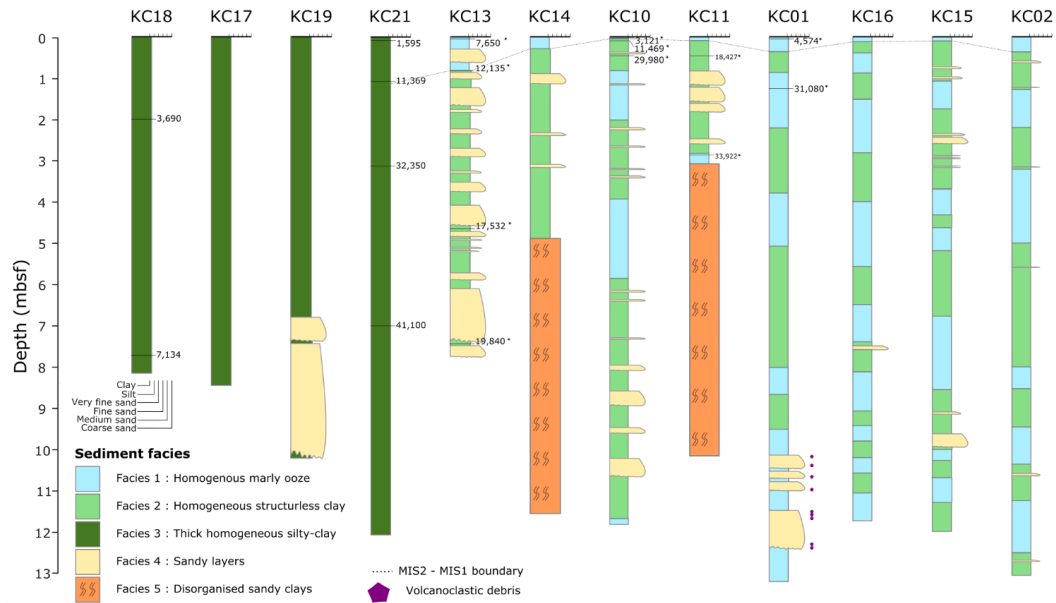
143



144 **Table 1: Core characteristics.**

Core	Depth (m)	Latitude	Longitude	Length (m)
KC01	3504	00°57,010' S	005°31,806' E	12,96
KC02	4109	00°13,525' S	004°07,620' E	12,76
KC10	3148	00°56,666' S	006°39,809' E	11,54
KC11	3372	00°52,008' S	006°00,008' E	9,92
KC13	2852	00°32,508' S	007°08,589' E	7,62
KC14	3140	00°25,010' S	006°36,006' E	11,34
KC15	3850	00°49,996' S	004°50,009' E	12,01
KC16	3738	01°05,003' S	004°52,010' E	11,48
KC17	565	00°51,188' S	008°29,377' E	8,20
KC18	366	01°01,940' S	008°25,409' E	7,99
KC19	1610	00°41,593' S	008°18,592' E	10,03
KC21	2347	00°13,004' S	008°00,011' E	11,81

145
 146
 147
 148



149

150 **Fig. 3: Sedimentological core logs from the Ogooue Fan, showing grain-size variation, lithology and bed thickness (location of**
 151 **cores are presented in Fig. 2). Ages are from ¹⁴C dating (dates with a star are from (Mignard et al., 2017).**

152

153 **4 Results**154 **4.1 Sedimentary facies**

155 The classification in five sedimentary facies used here is based on photography and X-ray imagery; grain size analyses and
156 CaCO₃ content (Fig. 3). Interpretation of these facies is based on the comparison with previous sedimentary facies
157 classifications such as (Normark and Damuth, 1997; Pickering et al., 1986; Stow and Piper, 1984).

158

159 *Facies 1: Homogenous, structureless marly ooze.* This facies is composed of structureless, light beige marly ooze with
160 relatively high concentration in planktonic foraminifers. The mean grain size is around 15 µm and the CaCO₃ content
161 ranges between 40 and 60 %. This facies is interpreted as a pelagic drape deposits; it forms the modern seafloor of the
162 deepest part of the Ogooue Fan and is observed in the majority of the cores top corresponding to the MIS 1 interval.

163 *Facies 2: Homogenous, structureless clay:* Facies 2 consists of dark brown clay. The mean grain size is less than 15 µm
164 and the CaCO₃ content is less than 30 %. This facies has been interpreted as hemipelagic drape deposits.

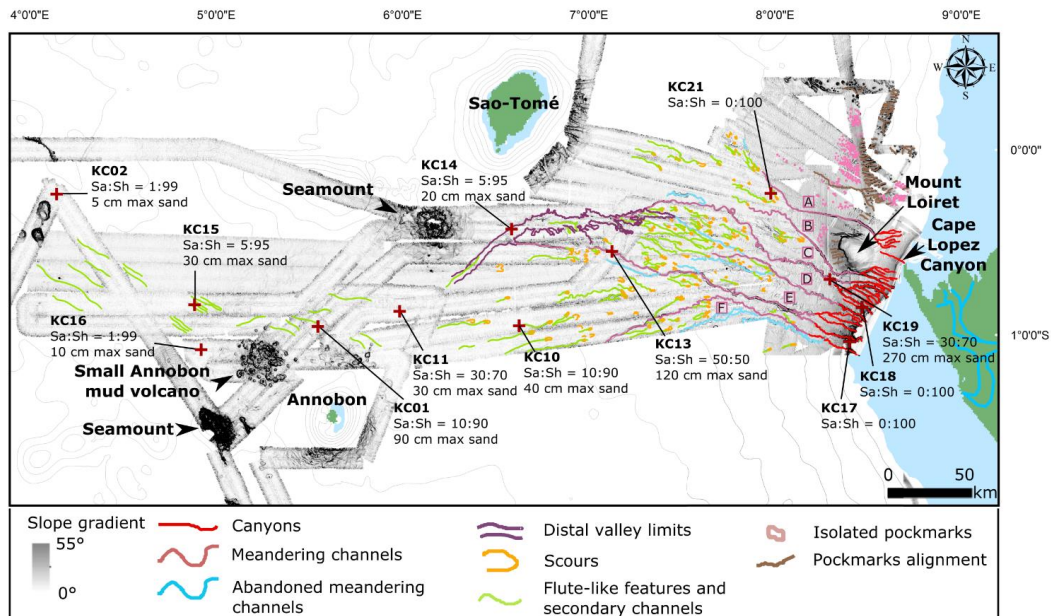
165 *Facies 3: Thick, homogeneous silty-clay:* Facies 3 consists of very thick homogeneous dark silt-clay layers containing less
166 than 10% of CaCO₃. This facies contains numerous quartz, micas and plant debris indicating a continental origin of the
167 sediments. It results from the deposition of the fine-grained suspended load coming from the Ogooue River and flowing
168 down the slope or belonging to the upper term of turbidite gravity flows.

169 *Facies 4: Silty to sandy layers:* Facies 4 consists of fine to medium sand beds with a thickness up to several meters. They
170 display a variety of bedding structures: normally-graded or massive. The composition varies from terrigenous (quartz and
171 mica) to biogenic (foraminifera), some sequences are highly enriched in organic debris (Mignard et al., 2017). They are
172 interpreted as being deposited by turbidity currents initiated on the Gabonese continental shelf. Four sequences samples in
173 core KC01 present a high concentration of volcanoclastic debris, such particles are completely absent of all the other
174 sequences (Fig. 3). This specific composition and the location of the core suggests that these sequences originate from the
175 close Annobon volcanic island.

176 *Facies 5: Disorganized sandy clays:* Facies 5 consists of thick intervals of deformed or chaotic clay with deformed or
177 folded silty to sandy layers. This facies is interpreted as resulting from mass transport deposits (slump or debris flow).



178 **4.2 Fan morphology**



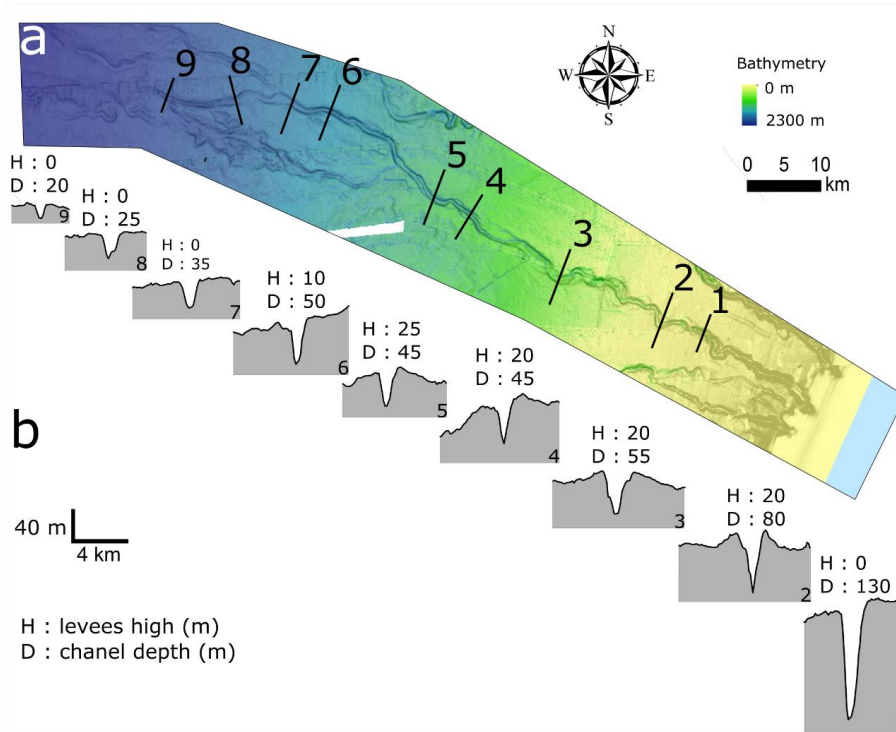
179

180 **Fig. 4: Interpreted gradient-shaded map of the Ogooue Fan showing the main features of the turbidite system. A, B, C, D, E and**
 181 **F are the six main channels discussed in the text. The sand/shale ratio of the cores are shown (Sa:Sh) as well as the maximum**
 182 **sand-bed thickness in each core (max sand).**

183 Analysis of the sub-surface data (bathymetry and acoustic imagery) reveals the different domains of the Ogooue
 184 sedimentary system and the different architectural features of the Ogooue Fan (Fig. 4).

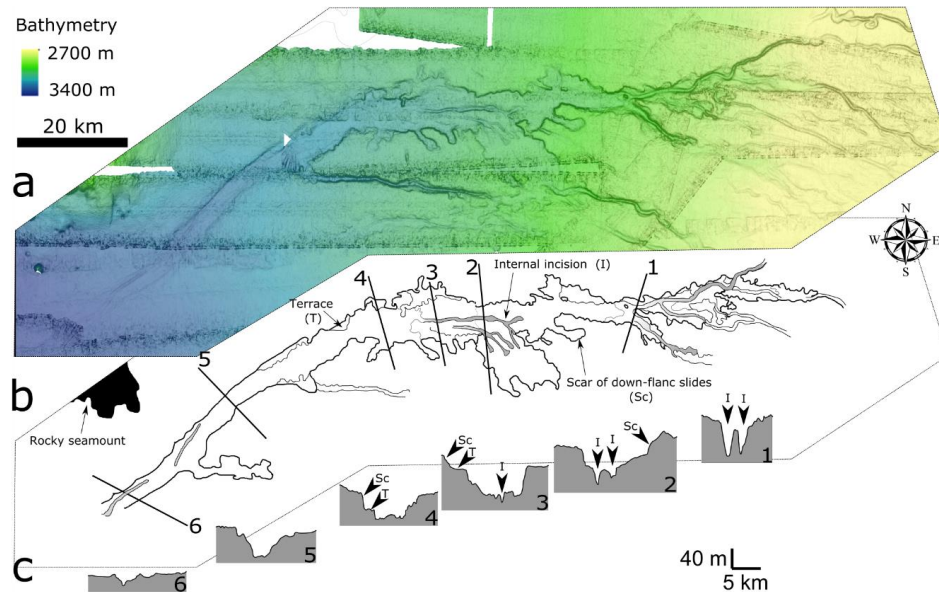
185 The Gabon shelf is relatively narrow decreasing in width from 60 to 5 km toward the Mandji Island. The slope is
 186 characterized by two main topographic elements: (1) the presence of the Mount Loiret, an inactive submarine volcano just
 187 west of the Manji Island, which forms a bathymetric obstacle on the upper slope and (2) a ramp of several tributary canyons
 188 located south of the Mount Loiret. This ramp is composed of ten major canyons, which deeply incise the shelf, and ten
 189 thinner and shallower incisions, which do not reach the shelf break. The continental shelf and the slope present low
 190 backscatter values except for the canyons, which appear with very-high backscatter value.

191 The transition between the continental slope and the continental rise, between 1,200 and 1,500 m water depth, is marked
 192 by a decrease in the slope gradient from more than 4% to 1.5%. At this water depth, several canyons merge to form five
 193 meandering channels (B to F in Fig. 4). These channels appear with higher backscatter value than the surrounding seafloor
 194 (Fig. 2b). These highly sinuous and meandering subparallel channel-levees complexes extend down to 2,200 m water depth
 195 with a general course oriented toward the north-west (Fig. 5). At 2,200 m water depth, the southernmost channel (channel
 196 F in Fig. 4) deviates its path toward the south-west.



197
 198 **Fig. 5: Detailed Bathymetric map of channel D (location in Fig. 2) and serial bathymetric profiles showing the evolution of the**
 199 **channel-levees along the slope.**

200 Downslope, on central part of the system, the seafloor located between 2,200 m and 2,500 m water depth, presents
 201 numerous erosional features like scours, lineations and secondary channels (Fig. 4). These erosional features appear on a
 202 very gentle slope area (0.6%) characterized by an heterogeneous medium backscatter facies (Fig. 2b). At 2,500 m water
 203 depth, just south of the Sao Tomé Island, the head of a large, 100 km-long, distal valley appears (Fig. 6). This valley can
 204 be divided in two parts of approximately equal length with two different orientations. The upper part of the valley is
 205 oriented E-W whereas the lower part is oriented NE-SW. This direction change is due to the presence of a rocky seamount
 206 located north of the valley and which deflects its course. The first half of the valley is up to 15 km wide with numerous
 207 erosional scars and terraces on its flanks. Its bottom, characterized by very high backscatter value, presents small internal
 208 erosion channels. Downstream, the valley becomes narrower with a “U” shape (Fig. 6, profile 5), its flanks appear regular
 209 with no scar of down-flank mass deposits. The depth of the valley decreases from 60 m in its central part to only 10 m near
 210 its mouth. The area located south of the distal valley is characterized by a heterogeneous low-backscatter facies. Some
 211 erosional features and secondary channels are present but scarce.



212
 213 **Fig. 6:** (a) Shaded bathymetry of the distal valley of the Ogooue Fan between 2,700 and 3,400 m water depth; (b) Interpretation
 214 of the main morphological features of the valley; (c) Six transverse profiles of the distal valley extracted from the bathymetry
 215 data.

216 West of the distal valley outlet, the seafloor is very flat and shows only subtle morphological variations except for local
 217 seamounts (rocky mounts and mud volcanoes). Few channel-like, narrow elongated depressions (maximum 10 m deep)
 218 presenting high backscatter values can be identified. These lineations are restrained to a long tongue of high backscatter
 219 that develops at the mouth of the valley (Fig. 2b, Detail A). This tongue is globally oriented E-W at the exit of the distal
 220 valley and then deflects toward the NW at 3,700 m water depth, following the steepest slope.

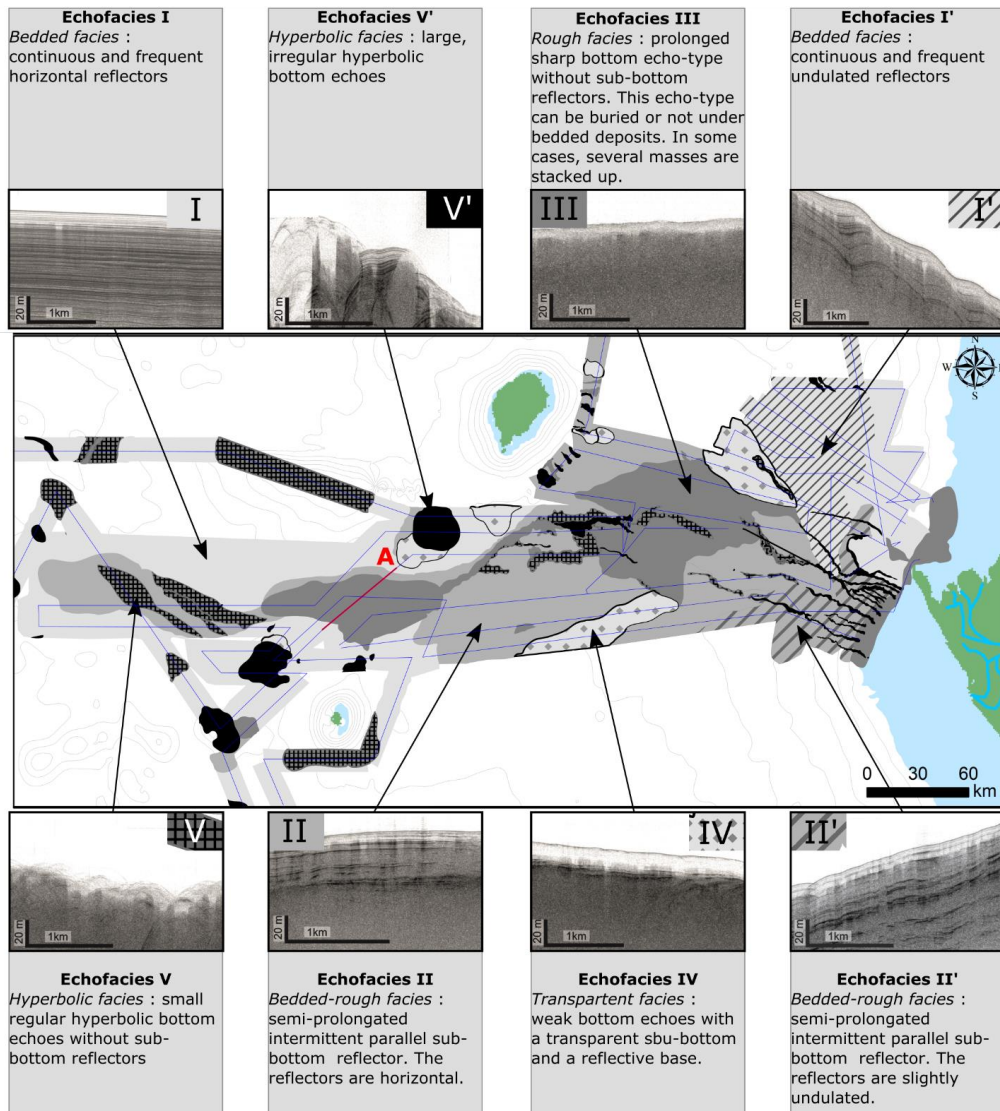
221 North of mount Loiret, the upper slope presents a lower slope gradient compared to the south part and is characterized by
 222 the presence of numerous linear pockmark trains on the upper part and random pockmarks fields on the lower part. These
 223 pockmarks have been previously described in (Pilcher and Argent, 2007). This whole area appears with a very low and
 224 homogeneous reflectivity. Trace of active sedimentation on this part of the margin is only visible in association with the
 225 Cape Lopez Canyon, which is the only canyon located north of the Mount Loiret. This canyon is associated with a small
 226 ponded lobe located just north of the Mount Loiret and referred as the Cape Lopez lobe (Biscara et al., 2011). This northern
 227 system is continued by Channel A which head is located in the vicinity of the Cape Lopez Lobe. At 2,200 m water depth,
 228 Channel A ends and its mouth is associated on the backscatter map with a fan-shaped area of very-high reflectivity which
 229 is associated with some secondary channels and erosional marks (Fig. 2b).

230
 231
 232
 233
 234



235 **4.3 Echofacies analysis and distribution**

236



237

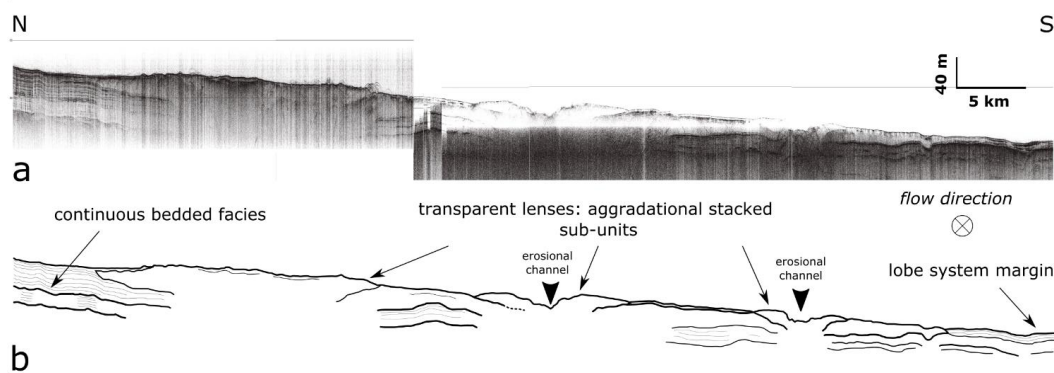
238 **Fig. 7 : Echofacies map of the Ogooue Fan. Each shade of grey represents a specific echofacies.**

239 Height main seismic facies have been discriminated on the profiles based on amplitude, frequency and geometry of the
 240 reflections (Fig. 7). They have been grouped into five main classes: (I) bedded, (II) bedded-rough, (III) rough, (IV)
 241 transparent and (V) hyperbolic. Although a few transitions between echofacies are sharp, most of them are gradual.

242 The echofacies of the edge of the Gabonese shelf consists of rough echofacies III (Fig. 7). Core KC18 indicates that this
 243 area is dominated by fine-grained terrigenous sedimentation.



244 North of the Mount Loiret, the continental slope presents bedded echofacies I which evolves into echofacies I' down isobath
 245 1,500 m which corresponds to an increase of the slope gradient. Bedded echofacies are commonly associated with
 246 hemipelagic sedimentation or with the alternation of hemipelagic sediments with gravity flow deposits (Damuth, 1980,
 247 1975; Loncke et al., 2009). The very low reflectivity of the area and the absence of any channel both suggest that only
 248 hemipelagic sedimentation occurs in this area. The wavy aspect of echofacies I' could be due to creeping.
 249 South of Mount Loiret, echofacies II and II' dominate on the continental slope. Despite the lack of sampling, the presence
 250 of semi-prolongated seismic reflectors can indicate the presence of coarse sediment. The echo-mapping of the continental
 251 rise reveals the presence of different facies. The central part, just upstream of the distal valley, is characterized by rough
 252 echofacies III that suggests the presence of coarse sediment. Some large channels are marked by hyperbolic facies certainly
 253 due to the irregular and steep seafloor. South of the distal valley, facies II dominates. Core KC10, collected in this area,
 254 indicates the alternation of clayey and sandy layer but with a predominance of fine-grained sediments (Fig. 3 Fig. 4).
 255 Echofacies IV is present in two main areas on the continental rise: they respectively form two lobe-shaped zones: one
 256 on the northern part, following the limits of the high-reflectivity area located at the mouth of channel A; the second in
 257 the southern part of the system in association with channel F. This echo-facies commonly corresponds to massive deposits
 258 without internal organization. Core KC21, collected in the northern area indicates homogeneous silty-clay sediments
 259 similar to those collected near the continental shelf.



260 **b**
 261 **Fig. 8 : a) Transverse 3.5 kHz seismic line and b) line drawing in the upper distal lobe area, see Fig. 7 for location of the line.**

262 On the abyssal plain, the area of the elongated tongue noticeable on the backscatter data presents different echofacies.
 263 Based on the 3.5 kHz profiles, it can be subdivided into two main domains. The upstream part, at the outlet of the distal
 264 valley, is characterized by rough echo character but with a specific organization: multiple aggradational stacked transparent
 265 sub-units from 10 to 30 meters thick are visible on the seismic lines (Fig. 8). This organization is characteristic of sandy
 266 lobes deposits. Core KC11, collected in this environment, presents several relatively-thick sandy layers and a several meter-
 267 thick disorganized sandy-clay sequence corresponding to slump deposit. The downstream part presents bedded-rough
 268 echofacies (II) associated with hyperbolic echofacies (V). Core KC15 shows mainly fine-grained sediments but recorded
 269 also several silty layers corresponding to the distalmost turbidite deposits.

270 On the edge of this tongue, high-penetration bedded facies (I) is dominant. The very continuous parallel bedding indicates
 271 hemipelagic sedimentation, which is confirmed by core KC16 and core KC02 both composed of alternating carbonate-rich
 272 and carbonate-poor clay sediments. Facies V' forms some patches on the seafloor and correspond to seafloor mounts such
 273 as mud volcanoes or rocky hills. The hyperbolic facies is due to the steep slopes and the irregular bathymetry.



274 Facies V and IV are also present forming lenses around the island of Sao-Tomé and Annobon. These features indicates
275 some downslope sedimentary transfer from these islands. The limited area covered by these facies suggests short transport
276 by sliding.

277

278

279

280

281

282

283

284

285

286

287

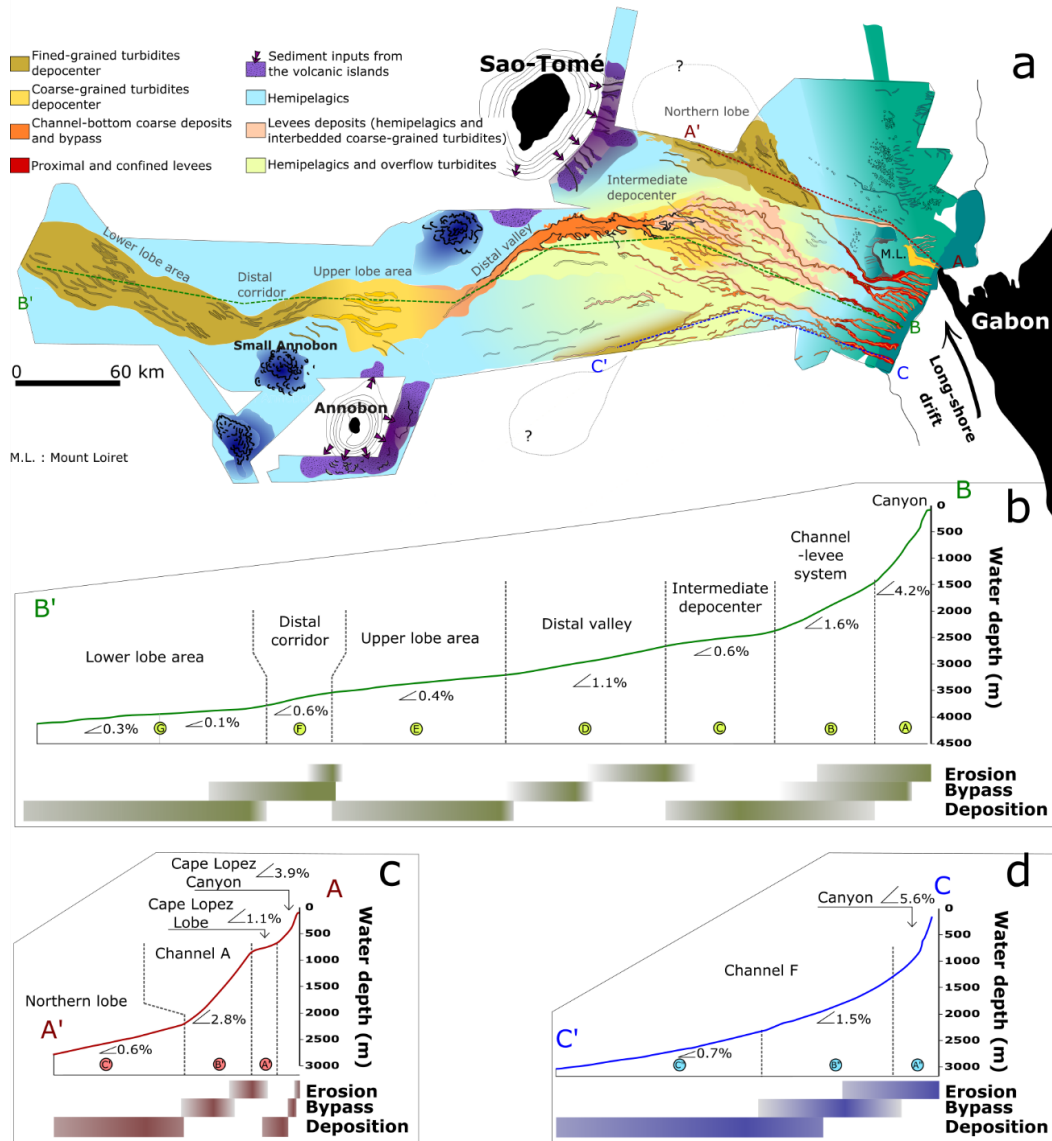
288

289



290 **5 Interpretation and discussion**

291 **5.1 Sedimentary processes along the fan**



292
 293 **Fig. 9:** a) Synthetic map showing the architecture and the recent sedimentary processes of the Ogooue Fan determined by
 294 imagery and echofacies mapping; b) c) and d) Longitudinal profiles from the bathymetric data along the central, northern and
 295 southern part of the Ogooue Fan. The differences in slope gradient along the transects are associated with the main sedimentary
 296 processes encountered along the slope.

297 The Ogooue turbidite system is a passive-margin delta-fed deep-sea turbidite system and correspond to a mature mud/sand-
 298 rich submarine fan according to the classification of (Reading and Richards, 1994). However, analysis of sub-surface data



299 (bathymetry, acoustic imagery and 3.5 kHz echo-characters) reveals a great variability of sediment processes in the
300 different domains of the margin, controlled mainly by the variations in the slope gradient and the presence of
301 seamounts(Fig. 9a).

302 Erosional processes seem to be predominant on the upper part of the slope as indicated by the presence of numerous straight
303 tributary canyons. Some of these canyons are deeply incised whereas others are much smaller. These characteristics can
304 indicate different ages for the canyons formations but also different types of formations processes. The morphology of the
305 smallest ones, which do not reach the shelf edge, indicates a formation by mass wasting and retrogressive erosion on the
306 continental slope, whereas the deep incision of the others can be due to erosion by turbidity currents sourced from the
307 continental shelf (Shepard, 1981). These two processes are not mutually exclusive and are probably contemporaneous
308 along the slope.

309 The transition from canyons to meandering channels with developed levees is related to a decrease in slope gradient. The
310 meandering channel-levees systems develops on a relative gentle slope from 1,500 to 2,200 m water depth. These channels
311 are mainly erosive on their central part while deposition occurs on their sides (Normark et al., 1993). The levees of the four
312 central channels (B, C, D and E in Fig. 2) show high reflectivity evidencing the occurrence of turbidite overflow processes.
313 The sinuosity of these channels is high in the upper segments and decreases westward (Fig. 5). Several studies have
314 documented that sinuosity of submarine channels increases with time (Babonneau et al., 2002; Deptuck et al., 2007, 2003;
315 Kolla, 2007; Peakall et al., 2000). The highly sinuous upper parts of the channels have consequently undergone a long
316 history whereas the distal straighter parts of the channels are in a more immature stage. Moreover, the height of the levees
317 and the depth of the channels both decrease in the lower parts of the system (Fig. 5). These morphological changes are due
318 to the slope that becomes gentler and progressively slows down the flow reducing its erosional power in the channel.
319 Simultaneously, deposition of fine particles by spilling of the upper part of the flow on the levees leads to a progressive
320 decrease of the fine-grained fraction transported by the channelized flows (Normark et al., 1993).

321 At 2,200 m water depth, the appearance of numerous erosional features such as isolated spoon-shaped scours, amalgamated
322 spoon-shaped scours erosional lineations and even secondary channel with tenuous surface expression are characteristic
323 of the channel lobe transition zone (Jegou et al., 2008; Kenyon et al., 1995; Mulder and Etienne, 2010; Wynn et al., 2007).
324 The appearance of these features correlates with a second abrupt decrease of the slope and with the transition from bedded-
325 rough to rough echo-facies indicating a change in the sedimentary process. This area corresponds to an unchannelized
326 deposition area referred as the intermediate depocenter in Fig. 9 and covering area surface of ca. 4,250 km². However, the
327 low penetration of the 3.5 kHz echosounder and the limited number of seismic lines in this area does not allow to obtain
328 an more detailed interpretation of the sedimentary processes in this part of the system.

329 The presence of a steeper slope downslope the intermediate depocenter led to the incision of the distal valley, which acts
330 as an outlet channel for turbidity currents that are energetic enough to travel through the previous flatter depositional area
331 (Fig. 9b). The upstream part of the valley is multi-sourced and migrates upstream by retrogressive erosion whereas the
332 downstream part appears more stable with a straighter pathway and steeper flanks. The pathway of the valley seems to be
333 highly controlled by the topography of the seafloor. This large distal valley corresponds to a single feeding “source” for
334 the lower fan and, consequently, the final depositional area is located downstream the valley. At the outlet of the distal
335 valley, the echofacies allows to distinguish an area mainly characterized by rough echofacies (III) forming stacked lenses.
336 This area, referred as the upper lobe area in Fig. 9, constitutes the main lobe complex of the Ogooue Fan. According to the
337 seismic data, this lobes depositional area is ~ 100 km long, reaches ~ 40 km in width, spreads over 2,860 km² and reaches
338 up to 40 m in thickness. The transparent lenses are interpreted as lobe elements and seem to be bounded by erosive bases



339 (Mulder and Etienne, 2010). Some incisions are imaged at the surface of the lobes; two of them are visible in Fig. 8. The
340 area where incisions are present is interpreted as the channelized part of the lobe. This lobe area presents a gentle slope
341 oriented north-south, suggesting that topographic compensation would shift southward the future lobe elements. However,
342 the few numbers of seismic lines does not allow to precise the internal geometry and the timing of the construction of the
343 different lobes units.

344 This depositional area is however not the distalmost part of the Ogooue Fan. Indeed, west of this lobe area, traces of active
345 sedimentation are visible on the reflectivity map (Fig. 2). The backscatter data shows high-backscatter finger-shape
346 structures organized like veins of a leaf suggesting perennial pathways of gravity flows (Fig. 2b, detail A). These lineations
347 are concentrated in a narrow 20 km wide corridor just west of the lobe area and then form a wider area extending up to
348 550 km offshore the Ogooue delta. This part of the system follows the same scheme as the one previously described
349 between the intermediate depocenter and the upper lobe area (Fig. 9b). Indeed the corridor appears on a segment of steeper
350 slope just at the downslope end of the upper lobe area. This corridor, which disappears when the slope becomes gentler,
351 was certainly formed by the repeated spill-over of the fine-grained top of turbidity currents over the upper lobe area. This
352 architecture suggests that this corridor is dominated by sediment erosion and transport. On the last segment with a very
353 low slope gradient sediment deposition dominates.

354 On the northern part of the slope, the isolated system composed of the Cape Lopez Canyon, Cape Lopez lobe, channel A
355 and northern lobe follows the same scheme (Fig. 9c). Indeed, the two successive depositional areas are located on an area
356 with a low slope-gradient whereas the erosion and bypass dominates on segments of steep slope-gradient.

357 In the southern part of the fan, channel F transports sediments southward. At 2,200 m water depth, a transparent echofacies
358 appears associated with the pathway of this channel. This echofacies suggests that sediment transported by this channel
359 might be partly deposited in this area by turbidity current overflow. This channel might also be associated with a
360 depositional lobe; however, the area covered by the MOCOSSED survey does not allow us to image it.

361 The Ogooue Fan presents a succession of depositional areas on segments with gentle slope (referred as 'steps' in (Smith,
362 2004)) and segments of steeper slope associated with erosion or bypass (Fig. 9). The depositional behavior in such system
363 is guided by an equilibrium profile of the system that creates preferential areas of sedimentation or erosion (Ferry et al.,
364 2005). Erosion is favored where local gradient increases, the eroded sediments being delivered downstream resulting in a
365 local increase in sediment load (Gee and Gawthorpe, 2006). This kind of fan geometry is common along the West African
366 margin where abrupt changes in slope gradient and complex seafloor morphology are inherited from salt tectonic movement
367 (Ferry et al., 2005; Gee et al., 2007; Gee and Gawthorpe, 2006; Pirmez et al., 2000). Moreover, in the case of the modern
368 Ogooue Fan and unlike the Congo and Niger systems, the presence of several bathymetric highs including the volcanic
369 islands of the Cameroon Volcanic Line and the different mud volcanoes constitute additional constraints for the flows.
370 These bathymetric highs deviate the pathways of different channels of the system as well as the pathway of the distal valley
371 and create several downslope depositional lobes. Such features are similar to the morphology of the Northwest African
372 margin where the Madeira, the Canary and the Cape Verde islands create a complex slope morphology (Masson, 1994;
373 Wynn et al., 2002, 2000). This specific topography controls the distribution of sedimentary facies along the Moroccan and
374 Mauritanian margin and creates several interconnected depositional basins similarly to the different depositional areas of
375 the Ogooue Fan.



376 5.2 Sedimentary facies distribution

377 The main sedimentary processes that are involved in the deposition of the Upper Quaternary sediment of the Ogooue
378 system are hemipelagic fall-out together with turbidity currents. Fine-grained pelagic/hemipelagic ‘background’
379 sedimentation is dominant across a large area of the margin, particularly on the lower rise and the adjacent basin plains.
380 These sediments are then overprinted by downslope gravity flows such as turbidity currents. However, the previously
381 described fan organization implies a specific repartition of the sedimentary facies and sand distribution within the system
382 (Fig. 4).

383 Cores collected in the upslope area (KC18 and KC17) show mostly hemipelagic sediments with a very low proportion of
384 carbonate. This reflects significant detrital flux associated with proximity to the Ogooue platform and influences of the
385 Ogooue river plume. Core KC19 collected down the slope just at the transition from canyon to channel-levees complexes
386 show two several meters-thick sandy sequences corresponding to top-cut-out Bouma sequences (Ta) interbedded with the
387 upper slope hemipelagites. These sandy turbidites, which are the thickest sand beds recorded in all the cores (Fig. 4),
388 indicate the occurrence of high-density turbidity currents flowing down the canyons. The lack of the upper terms of the
389 turbidite is consistent with deposition in the canyon of coarse-grains located at the base of the turbidity currents, whilst the
390 finer upper part of the current is transported downstream or spills over the levees. Levee deposits have been sampled by core
391 KC13, which shows numerous turbidites made up of centimeter-thick parallel or cross-bedded laminations of silt and fine
392 sands (Fig. 3). Unfortunately, no core has been collected directly in the intermediate depocenter. However, the rough
393 echofacies III found in this area associated with various erosional features suggest a high sand/shale ratio.

394 The distal valley certainly acts mainly as a conduit for the sediments, transporting them further downstream. However,
395 core KC14, collected on an internal terrace of the valley, shows that this valley is also an area of active sedimentation
396 notably due to down-flank sliding. The bottom of the valley could thus be composed of slump deposits and coarse-grained
397 sediments deposited by gravity flows. Downstream the distal valley, core KC11 shows that coarse-grained turbidites are
398 deposited in the first part of the lobe area. The abrupt transitions between erosional/bypass and depositional behavior
399 observed notably at the mouth of the distal valley is the result of hydraulic jumps affecting flows when they become
400 unconfined between channel sides and spread laterally (Garcia and Parker, 1989; Komar, 1971). Core KC15, located in the
401 lower lobe area, is composed of very thin silty turbidites corresponding to the upper terms of the Bouma sequence
402 interbedded with hemipelagic deposits. The upper lobe area certainly acts as a trap for the basal sand-rich parts of gravity
403 flows. Consequently, only the upper part of the flows, which is composed of fine-grained sediments, travels beyond this
404 area. The observed facies spatial distribution suggests a filling of the successive depocenters with a downslope decrease of
405 the coarse-grained sediment proportion (Fig. 4). The same facies distribution can be observed in the northern system.
406 Indeed, no sandy turbidites are recorded in KC21, only fine-grained sedimentation, whereas the study of cores taken in the
407 Cape Lopez lobe shows the presence of numerous sandy turbidite (Biscara et al., 2011). The Northern lobe is thus fed by
408 the downslope spilling of suspended fines transported at the top of turbidity currents flowing through the Cape Lopez
409 Canyon.

410 Whatever the current pathways are, the deposited material has a continental origin as suggested by the abundance of quartz,
411 micas and plant debris in the coarse-grained fraction. The important proportion of planktic foraminifers in the coarse-
412 grained fraction of turbidites located in the distal part of the system (core KC10- KC11- KC15) suggests that turbidity
413 currents previously eroded pelagic and hemipelagic deposits on the slopes located upflow where such deposits cover large
414 areas (Viana and Faugères, 1998). The presence of volcanoclastic debris in sandy layer found at the base of core KC01
415 suggests that sedimentary input may also come from the volcanic islands of Sao Tomé and Annobon. However, acoustic



416 data indicate that these inputs are limited to the close vicinity of the Sao-Tomé and Annobon islands. On the contrary to
417 the model proposed by (Wynn et al., 2000) for the Northwest African slope, the volcanic islands and other seamounts
418 present on the Ogooue turbidite system act mainly as obstacles for the flow pathway but are not important sediment
419 suppliers for the deep-sea system.

420 5.3 Palaeoceanographic control on the fan activity

421 The results of Mignard et al. (2017) concerning the study of five cores located along the central part of the Ogooue fan
422 showed that the fluvial sediments fed this part of the system almost only during times of relative low sea-level. This eustatic
423 control on the turbidite activity (switch on/off behavior) is classical for mid and low latitude passive margin fans where
424 canyon heads are detached from terrestrial sediment sources (e.g. Mississippi Fan (Bouma et al., 1989), Amazon Fan (Flood
425 and Piper, 1997), Rhone Fan (Lombo Tombo et al., 2015), Indus Fan (Kolla and Coumes, 1987)). Conversely,
426 sedimentation during periods of relative high sea-level such as the Holocene, is dominated by hemipelagic to pelagic fall-
427 out with a low part of fine terrigenous particles. Therefore, all cores collected in the central part of the system are capped
428 by 8 to 20 cm of light-brown nannofossil ooze corresponding to Holocene hemipelagic deposits (Fig. 3).

429 However, the northern part of the system appears to have a different behavior. (Biscara et al., 2011) showed that the Cape
430 Lopez lobe is currently recording both hemipelagic and turbidite sedimentation despite the present-day high sea-level. This
431 lobe is fed in sediment by the Cape Lopez Canyon, which incises the shelf up to the extremity of the Mandji Island (Biscara
432 et al., 2013). The deep incision of the continental shelf up to the coast combined with the longshore sediment transport
433 along the Mandji Island and the narrow shelf in this area (4 km wide) favor the capture of sediment by this canyon during
434 time of high sea-level (Biscara et al., 2013; Reyre, 1984). The northern lobe, which is directly connected to the Cape Lopez
435 lobe by Channel A, appears to be also fed by terrigenous sediments during the Holocene. Core KC21, located at the entrance
436 of the northern lobe, is entirely composed of *facies 3*, even for sediments deposited during MIS1 (Fig. 3).

437 In the Ogooue Fan system, the shelf width between the littoral area and the canyon heads is the main control factor on the
438 fan activity. During periods of relative low sea-level, the canyons of the central part of the system receive sediment from
439 the river system that extended across the subaerially exposed continental shelf. During periods of relative high sea-level,
440 river sediments are unable to reach the canyon heads south of the Manji Island and accumulate on the continental shelf
441 close to the Ogooue delta. However, part of these sediments mixed with sediments coming from the south Gabon margin
442 are drift-transported and contribute to supply the Cape Lopez canyon and consequently the Cape Lopez and Northern Lobe.
443 Due to their specific location and favorable hydrodynamic conditions on the shelf, sedimentation on the Cape Lopez and
444 the Northern lobes is active during relative sea-level highstands, on the contrary to the rest of the Ogooue Fan. This type
445 of supply is similar to the activity of the California margin where the La Jolla canyon is fed by drift-transported sediments
446 during highstand (Covault et al., 2011, 2007).

447 6 Conclusions

448 This study provides the first data on the morphology of the recent Ogooue deep-sea turbidite system and interpretations on
449 sedimentary processes occurring in this environment. The whole system is a mature, mud/sand rich submarine fan globally
450 organized upstream to downstream with canyons, then channel levee, then lobes. However, detailed study of acoustic data
451 proved that inherited paleo-topography and topographic features such as the Sao-Tomé and Annobon volcanic Islands and
452 other seamounts present in the area have significant effects on the distribution of sedimentary facies and morphological



453 elements of the system. The long-term interaction between gravity flows and the sea-floor topography have induced the
454 construction of successive depocenters and bypass areas. The gravity flows modified the topography according to a
455 theoretical equilibrium profile, eroding the seafloor when slopes are steeper than the theoretical equilibrium profiles and
456 depositing sediments when slopes are gentler than the theoretical equilibrium profile. Three successive sediment
457 depocenters have thus been identified along a longitudinal profile. They are associated with three areas of low slope
458 gradient. The two first deposition areas – the intermediate depocenter and the upper lobe area- recorded coarse-grained
459 sedimentation and are connected by a well-developed large distal valley measuring 100 km long. The distalmost depocenter
460 – the lower lobe area - received only the fine-grained portion of the sediment load that has bypassed the more proximal
461 deposit areas. The presence on the slope of the Mount Loiret has caused the formation of an isolated system composed of
462 the Cape Lopez canyon and lobe, which continues downstream by the Northern Lobe area.
463 The Ogooue Fan is currently in a low activity period since the recent Holocene rise of sea-level. Nowadays, the
464 sedimentation is mostly located on the Ogooue delta platform and on the upper slope. The turbidite system was most active
465 during the last glacial lowstand. Nonetheless, the northern part of the system appears to have an asynchronous activity with
466 the rest of the fan as this part is fed by the drift-transported sediments during time of relative high sea-level when the
467 activity in the rest of the system is shut-down.

468 7 Acknowledgments

469 We thank the SHOM (hydrological and oceanographic marine service) for the data, the ‘ARTEMIS’ technical platform for
470 radiocarbon age dating. We are also grateful to EPOC technicians and engineers: I. Billy, P. Lebleu, O. Ther and L.
471 Rossignol for the data acquisition.
472

473 8 References

- 474 Anka, Z., Séranne, M., Lopez, M., Scheck-Wenderoth, M., Savoye, B.: The long-term evolution of the Congo deep-sea
475 fan: A basin-wide view of the interaction between a giant submarine fan and a mature passive margin (ZaiAngo
476 project). *Tectonophysics* 470, 42–56. <https://doi.org/10.1016/j.tecto.2008.04.009>, 2009.
- 477 Babonneau, N., Savoye, B., Cremer, M., Klein, B.: Morphology and architecture of the present canyon and channel system
478 of the Zaire deep-sea fan. *Mar. Pet. Geol.* 19, 445–467. [https://doi.org/10.1016/S0264-8172\(02\)00009-0](https://doi.org/10.1016/S0264-8172(02)00009-0), 2002.
- 479 Biscara, L., Mulder, T., Hanquiez, V., Marieu, V., Crespín, J.-P., Braccini, E., Garlan, T.: Morphological evolution of Cap
480 Lopez Canyon (Gabon): Illustration of lateral migration processes of a submarine canyon. *Mar. Geol.* 340, 49–
481 56. <https://doi.org/10.1016/j.margeo.2013.04.014>, 2013.
- 482 Biscara, L., Mulder, T., Martinez, P., Baudin, F., Etcheber, H., Jouanneau, J.-M., Garlan, T.: Transport of terrestrial organic
483 matter in the Ogooué deep sea turbidite system (Gabon). *Mar. Pet. Geol.* 28, 1061–1072.
484 <https://doi.org/10.1016/j.marpetgeo.2010.12.002>, 2011.
- 485 Bouma, A.H., Coleman, J.M., Stelling, C.E., Kohl, B.: Influence of relative sea level changes on the construction of the
486 Mississippi Fan. *Geo-Mar. Lett.* 9, 161–170. <https://doi.org/10.1007/BF02431043>, 1989.
- 487 Bourgoin, J., Reyre, D., Magloire, P., Krichewsky, M.: Les canyons sous-marins du cap Lopez (Gabon). *Cah Ocean.* 6,
488 372–387, 1963.
- 489 Brownfield, M.E., Charpentier, R.R.: Geology and total petroleum systems of the West-Central Coastal Province (7203),
490 West Africa. *US Geol. Surv. Bull.* 2207-B, 52, 2006.
- 491 Cameron, N.R., White, K.: Exploration Opportunities in Offshore Deepwater Africa. IBC ‘Oil Gas Dev. West Afr. Lond.
492 UK, 1999.
- 493 Covault, J.A., Normark, W.R., Romans, B.W., Graham, S.A.: Highstand fans in the California borderland: The overlooked
494 deep-water depositional systems. *Geology* 35, 783. <https://doi.org/10.1130/G23800A.1>, 2007.



- 495 Covault, J.A., Romans, B.W., Graham, S.A., Fildani, A., Hilley, G.E.: Terrestrial source to deep-sea sink sediment budgets
 496 at high and low sea levels: Insights from tectonically active Southern California. *Geology* 39, 619–622.
 497 <https://doi.org/10.1130/G31801.1>, 2011.
- 498 Damuth, J.E.: Use of high-frequency (3.5–12 kHz) echograms in the study of near-bottom sedimentation processes in the
 499 deep-sea: a review. *Mar. Geol.* 38, 51–75, 1980.
- 500 Damuth, J.E.: Echo character of the western equatorial Atlantic floor and its relationship to the dispersal and distribution
 501 of terrigenous sediments. *Mar. Geol.* 18, 17–45. [https://doi.org/10.1016/0025-3227\(75\)90047-X](https://doi.org/10.1016/0025-3227(75)90047-X), 1975.
- 502 Damuth, J.E., Hayes, D.E.: Echo character of the East Brazilian continental margin and its relationship to sedimentary
 503 processes. *Mar. Geol.* 24, 73–95. [https://doi.org/10.1016/0025-3227\(77\)90002-0](https://doi.org/10.1016/0025-3227(77)90002-0), 1977.
- 504 Deptuck, M.E., Steffens, G.S., Barton, M., Pirmez, C.: Architecture and evolution of upper fan channel-belts on the Niger
 505 Delta slope and in the Arabian Sea. *Mar. Pet. Geol.* 20, 649–676.
 506 <https://doi.org/10.1016/j.marpetgeo.2003.01.004>, 2003.
- 507 Deptuck, M.E., Sylvester, Z., Pirmez, C., O’Byrne, C.: Migration–aggradation history and 3-D seismic geomorphology of
 508 submarine channels in the Pleistocene Benin-major Canyon, western Niger Delta slope. *Mar. Pet. Geol.* 24, 406–
 509 433. <https://doi.org/10.1016/j.marpetgeo.2007.01.005>, 2007.
- 510 Droz, L., Marsset, T., Ondras, H., Lopez, M., Savoye, B., Spy-Anderson, F.-L.: Architecture of an active mud-rich turbidite
 511 system: The Zaire Fan (Congo–Angola margin southeast Atlantic): Results from ZaAngo 1 and 2 cruises. *AAPG*
 512 *Bull.* 87, 1145–1168, 2003.
- 513 Droz, L., Rigaut, F., Cochonat, P., Tofani, R.: Morphology and recent evolution of the Zaire turbidite system (Gulf of
 514 Guinea). *GSA Bull.* 108, 253–269. [https://doi.org/10.1130/0016-7606\(1996\)108<108:MAREOT>2.3.CO;2](https://doi.org/10.1130/0016-7606(1996)108<108:MAREOT>2.3.CO;2), 1996.
- 516 Ferry, J.-N., Mulder, T., Parize, O., Raillard, S.: Concept of equilibrium profile in deep-water turbidite system: effects of
 517 local physiographic changes on the nature of sedimentary process and the geometries of deposits. *Geol. Soc. Lond.*
 518 *Spec. Publ.* 244, 181–193. <https://doi.org/10.1144/GSL.SP.2005.244.01.11>, 2005.
- 519 Flood, R.D., Piper, D.J.W.: Amazon Fan sedimentation: the relationship to equatorial climate change, continental
 520 denudation, and sea-level fluctuations., in: Flood, R.D., Piper, D.J.W., Klaus, A., Peterson, L.C. (Eds.),
 521 *Proceeding of the Ocean Drilling Program, Scientific Results*. pp. 653–675, 1997.
- 522 Garcia, M., Parker, G.: Experiments on hydraulic jumps in turbidity currents near a canyon-fan transition. *Science* 245,
 523 393–396. <https://doi.org/10.1126/science.245.4916.393>, 1989.
- 524 Gay, A., Lopez, M., Cochonat, P., Sultan, N., Cauquil, E., Brigaud, F.: Sinuous pockmark belt as indicator of a shallow
 525 buried turbiditic channel on the lower slope of the Congo basin, West African margin. *Geol. Soc. Lond. Spec.*
 526 *Publ.* 216, 173–189. <https://doi.org/10.1144/GSL.SP.2003.216.01.12>, 2003.
- 527 Gee, M.J.R., Gawthorpe, R.L.: Submarine channels controlled by salt tectonics: Examples from 3D seismic data offshore
 528 Angola. *Mar. Pet. Geol.* 23, 443–458. <https://doi.org/10.1016/j.marpetgeo.2006.01.002>, 2006.
- 529 Gee, M.J.R., Gawthorpe, R.L., Bakke, K., Friedmann, S.J.: Seismic Geomorphology and Evolution of Submarine Channels
 530 from the Angolan Continental Margin. *J. Sediment. Res.* 77, 433–446. <https://doi.org/10.2110/jsr.2007.042>, 2007.
- 531 Giresse, P.: Carte sédimentologique des fonds sous-marins du delta de l’Ogooué, 1969.
- 532 Giresse, P., Odin, G.S.: Nature minéralogique et origine des glauconies du plateau continental du Gabon et du Congo.
 533 *Sedimentology* 20, 457–488, 1973.
- 534 Guillou, R.: MOCOSSED 2010 croise, Pourquoi pas ? R/V. <https://doi.org/10.17600/10030110>, 2010.
- 535 Hanquiez, V., Mulder, T., Lecroart, P., Gonthier, E., Marchès, E., Voisset, M.: High resolution seafloor images in the Gulf
 536 of Cadiz, Iberian margin. *Mar. Geol.* 246, 42–59. <https://doi.org/10.1016/j.margeo.2007.08.002>, 2007.
- 537 Heezen, B.C., Menzies, R.J., Schneider, E.D., Ewing, W.M., Granelli, N.C.L.: Congo submarine canyon. *AAPG Bull.* 48,
 538 1126–1149, 1964.
- 539 Jansen, J.H.F., Van Weering, T.C.E., Gieles, R., Van Iperen, J.: Middle and late Quaternary oceanography and climatology
 540 of the Zaire-Congo fan and the adjacent eastern Angola Basin. *Neth. J. Sea Res.* 17, 201–249, 1984.
- 541 Jegou, I., Savoye, B., Pirmez, C., Droz, L.: Channel-mouth lobe complex of the recent Amazon Fan: The missing piece.
 542 *Mar. Geol.* 252, 62–77. <https://doi.org/10.1016/j.margeo.2008.03.004>, 2008.
- 543 Kenyon, N.H., Millington, J., Droz, L., Ivanov, M.K.: Scour holes in a channel-lobe transition zone on the Rhône Cone,
 544 in: *Atlas of Deep Water Environments*. Springer, Dordrecht, pp. 212–215. https://doi.org/10.1007/978-94-011-1234-5_31, 1995.
- 546 Kolla, V.: A review of sinuous channel avulsion patterns in some major deep-sea fans and factors controlling them. *Mar.*
 547 *Pet. Geol.* 24, 450–469. <https://doi.org/10.1016/j.marpetgeo.2007.01.004>, 2007.
- 548 Kolla, V., Coumes, F.: Morphology, Internal Structure, Seismic Stratigraphy, and Sedimentation of Indus Fan. *AAPG Bull.*
 549 71, 650–677, 1987.
- 550 Komar, P.D.: Hydraulic jumps in turbidity currents. *Bull. Geol. Soc. Am.* 82, 1477–1488. [https://doi.org/10.1130/0016-7606\(1971\)82\[1477:HJITC\]2.0.CO;2](https://doi.org/10.1130/0016-7606(1971)82[1477:HJITC]2.0.CO;2), 1971.
- 552 Lérique, J., Barret, J., Walter, R.: Hydrographie, hydrologie, in: *Géographie et cartographie du Gabon: atlas illustré*.
 553 EDICEF, Paris, pp. 14–17, 1983.



- 554 Lombo Tombo, S., Dennielou, B., Berné, S., Bassetti, M.-A., Toucanne, S., Jorry, S.J., Jouet, G., Fontanier, C.: Sea-level
 555 control on turbidite activity in the Rhone canyon and the upper fan during the Last Glacial Maximum and Early
 556 deglacial. *Sediment. Geol.* 323, 148–166. <https://doi.org/10.1016/j.sedgeo.2015.04.009>, 2015.
- 557 Loncke, L., Droz, L., Gaullier, V., Basile, C., Patriat, M., Roest, W.: Slope instabilities from echo-character mapping along
 558 the French Guiana transform margin and Demerara abyssal plain. *Mar. Pet. Geol.* 26, 711–723.
 559 <https://doi.org/10.1016/j.marpetgeo.2008.02.010>, 2009.
- 560 Lonergan, L., Jamin, N.H., Jackson, C.A.-L., Johnson, H.D.: U-shaped slope gully systems and sediment waves on the
 561 passive margin of Gabon (West Africa). *Mar. Geol.* 337, 80–97. <https://doi.org/10.1016/j.margeo.2013.02.001>,
 562 2013.
- 563 Mahé, G., Lérique, J., Olivry, J.-C.: Le fleuve Ogooué au Gabon : reconstitution des débits manquants et mise en évidence
 564 de variations climatiques à l'équateur. *Hydrol Cont.* 5, 105–124, 1990.
- 565 Masson, D.G.: Late Quaternary turbidity current pathways to the Madeira Abyssal Plain and some constraints on turbidity
 566 current mechanisms. *Basin Res.* 6, 17–33. <https://doi.org/10.1111/j.1365-2117.1994.tb00072.x>, 1994.
- 567 Migeon, S., Weber, O., Faugetes, J.-C., Saint-Paul, J.: SCOPIX: a new X-ray imaging system for core analysis. *Geo-Mar.*
 568 *Lett.* 18, 251–255, 1998.
- 569 Mignard, S.L.-A., Mulder, T., Martinez, P., Charlier, K., Rossignol, L., Garlan, T.: Deep-sea terrigenous organic carbon
 570 transfer and accumulation: Impact of sea-level variations and sedimentation processes off the Ogooué River
 571 (Gabon). *Mar. Pet. Geol.* 85, 35–53. <https://doi.org/10.1016/j.marpetgeo.2017.04.009>, 2017.
- 572 Mougamba, R.: Chronologie et architecture des systems turbiditiquest Cénozoïques du Prisme sédimentaire de l'Ogooué
 573 (Marge Nord-Gabon). Université de Lille, Lille, 1999.
- 574 Mouscardes, P.: OPTIC CONGO 2 croise, RV Beaupré
 575 <http://campagnes.flotteoceanographique.fr/campagnes/5090050/fr/>, 2005.
- 576 Mulder, T., Etienne, S.: Lobes in deep-sea turbidite systems: State of the art. *Sediment. Geol.* 229, 75–80.
 577 <https://doi.org/10.1016/j.sedgeo.2010.06.011>, 2010.
- 578 Normark, W.R., Damuth, J.E.: Sedimentary facies and associated depositional elements of the Amazon Fan, Proceedings
 579 of the Ocean Drilling Program. Ocean Drilling Program. <https://doi.org/10.2973/odp.proc.sr.155.1997>, 1997.
- 580 Normark, W.R., Posamentier, H., Mutti, E.: Turbidite systems: State of the art and future directions. *Rev. Geophys.* 31,
 581 91–116. <https://doi.org/10.1029/93RG02832>, 1993.
- 582 Olausson, E.: Oxygen and carbon isotope analyses of a late quaternary core in the Zaire (Congo) fan. *Neth. J. Sea Res.* 17,
 583 276–279. [https://doi.org/10.1016/0077-7579\(84\)90050-4](https://doi.org/10.1016/0077-7579(84)90050-4), 1984.
- 584 Peakall, J., McCaffrey, B., Kneller, B.: A process model for the evolution, morphology, and architecture of sinuous
 585 submarine channels. *J. Sediment. Res.* 70, 434–448, 2000.
- 586 Pickering, K., Stow, D., Watson, M., Hiscott, R.: Deep-water facies, processes and models: a review and classification
 587 scheme for modern and ancient sediments. *Earth Sci. Rev.* 23, 75–174. [https://doi.org/10.1016/0012-8252\(86\)90001-2](https://doi.org/10.1016/0012-8252(86)90001-2), 1986.
- 588
- 589 Pilcher, R., Argent, J.: Mega-pockmarks and linear pockmark trains on the West African continental margin. *Mar. Geol.*
 590 244, 15–32. <https://doi.org/10.1016/j.margeo.2007.05.002>, 2007.
- 591 Pirmez, C., Beaubouef, R.T., Friedmann, S.J., Mohrig, D.C.: Equilibrium Profile and Baselevel in Submarine Channels:
 592 Examples from Late Pleistocene Systems and Implications for the Architecture of Deepwater Reservoirs, in:
 593 Weimer, P. (Ed.), *Deep-Water Reservoirs of the World*. <https://doi.org/10.5724/gcs.00.20>, 2000.
- 594 Reading, H.G., Richards, M.: Turbidite systems in deep-water basin margins classified by grain size and feeder system.
 595 *AAPG Bull.* 78, 792–822, 1994.
- 596 Reyre, D.: Evolution géologique et caractères pétroliers d'une marge passive: cas du bassin du Bas Congo–Gabon. *Bull.*
 597 *Cent. Rech. Explor. Prod. Elf Aquitaine* 8, 303–332, 1984.
- 598 Séranne, M., Abeigne, C.-R.N.: Oligocene to Holocene sediment drifts and bottom currents on the slope of Gabon
 599 continental margin (west Africa): Consequences for sedimentation and southeast Atlantic upwelling. *Sediment.*
 600 *Geol.* 128, 179–199, 1999.
- 601 Séranne, M., Anka, Z.: South Atlantic continental margins of Africa: A comparison of the tectonic vs climate interplay on
 602 the evolution of equatorial west Africa and SW Africa margins. *J. Afr. Earth Sci.* 43, 283–300.
 603 <https://doi.org/10.1016/j.jafrearsci.2005.07.010>, 2005.
- 604 Séranne, M., Bruguier, O., Moussavou, M.: U-Pb single zircon grain dating of Present fluvial and Cenozoic aeolian
 605 sediments from Gabon: consequences on sediment provenance, reworking, and erosion processes on the equatorial
 606 West African margin. *Bull. Société Géologique Fr.* 179, 29–40, 2008.
- 607 Shepard, F.P.: Submarine Canyons: Multiple Causes and Long-Time Persistence. *AAPG Bull.* 65.
 608 <https://doi.org/10.1306/03B59459-16D1-11D7-8645000102C1865D>, 1981.
- 609 Smith, R.: Silled sub-basins to connected tortuous corridors: sediment distribution systems on topographically complex
 610 sub-aqueous slopes. *Geol. Soc. Lond. Spec. Publ.* 222, 23–43. <https://doi.org/10.1144/GSL.SP.2004.222.01.03>,
 611 2004.
- 612 Stow, D.A.V., Piper, D.J.W.: Deep-water fine-grained sediments: facies models. *Geol. Soc. Lond. Spec. Publ.* 15, 611–
 613 646. <https://doi.org/10.1144/GSL.SP.1984.015.01.38>, 1984.



- 614 Syvitski, J.P.M., Vörösmarty, C.J., Kettner, A.J., Green, P.: Impact of Humans on the Flux of Terrestrial Sediment to the
615 Global Coastal Ocean. *Science* 308, 376–380. <https://doi.org/10.1126/science.1109454>, 2005.
- 616 Unterseh, S.: Cartographie et caractérisation du fond marin par sondeur multifaisceaux. Vandoeuvre-les-Nancy, INPL,
617 1999.
- 618 Viana, A.R., Faugères, J.-C.: Upper slope sand deposits: the example of Campos Basin, a latest Pleistocene-Holocene
619 record of the interaction between alongslope and downslope currents. *Geol. Soc. Spec. Publ.* 129, 287–316.
620 <https://doi.org/10.1144/GSL.SP.1998.129.01.18>, 1998.
- 621 Volat, J.-L., Pastouret, L., Vergnaud-Grazzini, C.: Dissolution and carbonate fluctuations in Pleistocene deep-sea cores: A
622 review. *Mar. Geol.* 34, 1–28. [https://doi.org/10.1016/0025-3227\(80\)90138-3](https://doi.org/10.1016/0025-3227(80)90138-3), 1980.
- 623 Weering, T.C.E. van, Iperen, J. van: Fine-grained sediments of the Zaire deep-sea fan, southern Atlantic Ocean. *Geol. Soc.*
624 *Lond. Spec. Publ.* 15, 95–113. <https://doi.org/10.1144/GSL.SP.1984.015.01.06>, 1984.
- 625 Wonham, J., Jayr, S., Mougamba, R., Chuilon, P.: 3D sedimentary evolution of a canyon fill (Lower Miocene-age) from
626 the Mandorve Formation, offshore Gabon. *Mar. Pet. Geol.* 17, 175–197. [https://doi.org/10.1016/S0264-](https://doi.org/10.1016/S0264-8172(99)00033-1)
627 [8172\(99\)00033-1](https://doi.org/10.1016/S0264-8172(99)00033-1), 2000.
- 628 Wynn, R.B., Cronin, B.T., Peakall, J.: Sinuous deep-water channels: Genesis, geometry and architecture. *Mar. Pet. Geol.*
629 24, 341–387. <https://doi.org/10.1016/j.marpetgeo.2007.06.001>, 2007.
- 630 Wynn, R.B., Masson, D.G., Stow, D.A., Weaver, P.P.: The Northwest African slope apron: a modern analogue for deep-
631 water systems with complex seafloor topography. *Mar. Pet. Geol.* 17, 253–265. [https://doi.org/10.1016/S0264-](https://doi.org/10.1016/S0264-8172(99)00014-8)
632 [8172\(99\)00014-8](https://doi.org/10.1016/S0264-8172(99)00014-8), 2000.
- 633 Wynn, R.B., Weaver, P.P.E., Masson, D.G., Stow, D.A.V.: Turbidite depositional architecture across three interconnected
634 deep-water basins on the north-west African margin. *Sedimentology* 49, 669–695. [https://doi.org/10.1046/j.1365-](https://doi.org/10.1046/j.1365-3091.2002.00471.x)
635 [3091.2002.00471.x](https://doi.org/10.1046/j.1365-3091.2002.00471.x), 2002.
- 636 Zachariasse, W.J., Schmidt, R.R., Van Leeuwen, R.J.W.: Distribution of Foraminifera and calcareous nannoplankton in
637 Quaternary sediments of the eastern Angola Basin in response to climatic and oceanic fluctuations. *Neth. J. Sea*
638 *Res.* 17, 250–275, 1984.
- 639